Thermal and electric performances of roll-bond flat plate applied to conventional PV modules for heat recovery

Paola Bombarda, Gioele Di Marcoberardino, Andrea Lucchini, Sonia Leva, Giampaolo Manzolini *, Luca Molinaroli, Federico Pedranzini, Riccardo Simonetti

Politecnico di Milano, Dipartimento di Energia, Via Lambruschini 4, 20156 Milano, Italy[1]

Photovoltaic thermal (PVT) modules can increase the renewable energy production by combining the electricity and heat generation. PVT are seen as promising technology for residential applications where the heat can be exploited on site. In this work, the performances of three different PVT modules are eval-uated in real operating conditions at the SolarTech^{LAB}. Performance evaluation is conducted both by means of conventional and innovative performance indexes (corrected thermal efficiency and second law efficiency) which are expressly introduced in this work to take into account PVT peculiarities. Dedicated experiments outlined the importance of adopting these peculiar indexes when comparing dif-ferent PVT modules. In terms of heat recovered, the best roll-bond configuration increases the thermal efficiency by 8% points with respect to the conventional sheet-and-tube one. PVT modules have lower thermal efficiency than commercial only thermal modules (41% vs. 55%), however, the second law efficiency outlines the advantages of producing electricity and heat instead of only heat (16% vs. 2%).

Keywords:
Photovoltaic thermal
Thermal efficiency
Electric efficiency
First law efficiency
Second law efficiency

Nomenclature

A	panel area [m^2]
A_{AC}	alternating current intensity [A]
c	specific water heat capacity [4.186 kJ kg^{-1} K^{-1}]
D_p	panel thickness [m]
$E_{EL,TOT}$	overall electric energy produced [kW h]
$E_{TH,TOT}$	overall thermal energy recovered [kW h]
G	solar irradiance [W m^{-2}]
I_{max}	maximum current for the energy meter [A]
I_{TOT}	overall yearly solar irradiance [kW h/m^2 y^{-1}]
K	overall heat transfer coefficient [W m^{-2} K^{-1}]
N	number of samples
P_{el}	electric power [W]
$\dot{Q}_{th}$	heat transfer rate [W]
T	temperature [°C]
u	relative uncertainty [%]
U	absolute uncertainty
U_B	absolute uncertainty measurements (type B)
$\dot{V}$	volumetric flow rate [m^3 s^{-1}]
V_{AC}	alternating current voltage [V]
V_N	nominal voltage [V]
W_p	rated electric power [W]

Acronyms

IAM	Incidence Angle Modifier
PES	Primary Energy Savings
PV	Photovoltaic panel
PVT	Photovoltaic/thermal collector
RB	Roll-Bond type panel
REF	Reference panel
RES	Renewable Energy Sources

Greek letters

Γ	intercept factor [°]
ρ	density [kg m^{-3}]
η	efficiency [%]
σ_{st}	standard deviation measurements

Subscripts

amb	ambient
el	electric
in	panel inlet
m	mean
opt	optical
out	panel outlet
ref	reference
th	thermal
I	first law
II	second law
LMTD	mean logarithmic temperature difference
0	thermal efficiency at null reduced temperature

* Corresponding author.
E-mail address: giampaolo.manzolini@polimi.it (G. Manzolini).
[1] www.solartech.polimi.it.

Published Journal Article available at: http://dx.doi.org/10.1016/j.applthermaleng.2016.05.172

1. Introduction

The electricity produced by renewable energy sources (RES) is constantly increasing world-wide thanks to government policies and technological advancements. Europe has experienced one of the largest RES growths: in the last five years the electricity generation by RES, and in particularly by photovoltaic and wind plants, has doubled. Photovoltaic has seen a significant grow thanks to government subsidies in many country of the world (i.e. Italy, Germany) and to the production cost reduction, and consequently the price.

Commercial PV electric efficiency is quite low, usually in the range between 5% for thin film and 20% for monocrystalline; hence most of the incoming solar energy is lost [1].

In order to further increase the energy recovered from the sun, a heat recovery system on the back-sheet of the panel can be installed leading to the so-called photovoltaic/thermal (PVT) collector concept.

The attractive feature of the PVT collectors are largely discussed in many pioneering and review studies [2–5] and can be summarized as follow:

- The same system has two useful outputs, with further energy savings and potential pay-back time reduction. Moreover, the overall electricity and heat produced by PVT panels is higher than the sum of electricity and heat produced by two conventional separate photovoltaic and thermal collectors having the same aperture area as the PVT collector;
- Higher solar energy exploitation means lower footprint which can be important in roof with limited space available;
- PV cells work at lower temperatures with higher efficiency;
- The thermal power can be used both for space heating and cooling (post-heating or desiccant wheels) depending on the season;
- It can be easily retrofitted.

Expected average yearly efficiency (electric plus thermal efficiency) were calculated in the range of 34–39% [2] with instantaneous values up to 50% [6,7], being the reference PV electric efficiency in the range of 15%. Due to its superior performance over traditional PV or thermal collector, the PVT technology has received a great deal of attention over years as demonstrated by many recent review works [8–11]. Advanced design of the absor-ber plate [9], development of concentrator-type PVT [11], integra-tion with heat pumps [8] and integration with the building envelope [10] are generally recommended as the directions where research efforts have to be focused to reduce the PVT collector losses and pushing the overall efficiency to the highest value. The use of a liquid coolant such as water guarantees a more uniform temperature of the PV cells compared to the adoption of air and the highest efficiencies [12]. In recent advancement, a refrigerant is used to cool the PV module to exploit its full potentiality in a solar driven heat pumps [13].

With respect to the heat recovery system, Zondag [2] compared different heat recovery configurations (sheet and tube collector, channel PVT collector, free-flow PVT collectors and two absorber PVT-collector) based on analytical models and experimental validation of the electric and thermal efficiencies. Results showed that only one configuration (sheet and tube with uncovered PV) has a higher electric efficiency than reference PV modules but the annual thermal efficiency is just 24%. Improved configurations can increase the thermal efficiency up to 39% with penalties in terms of electric efficiencies. Chow [8] in his review concluded that the optimal design of any PVT system depends on the selected application and on the location. Dupeyrat et al. [14] developed an improved lamination process that allowed to increase the generated current density of 2 mA cm^{-2} with respect to conventional lamination process. A prototype of PVT collector was furtherly built using a roll-bond as absorber. The solar panel is tested using an indoor solar simulator and an overall efficiency as high as 87% is achieved. Kim and Kim [15] measured the performance of a sheet-and-tube PVT collector finding that the overall efficiency achieves 66%. Aste et al. [16] modeled and measured the perfor-mances of PV modules with glass cover and roll-bond flat plate absorber. The measured thermal efficiency was 28.2% which is a promising results since it was determined in winter time. Allan et al. [17] experimentally measured the performances of PVT pan-els built by placing the PV laminates on the top of an aluminum sheet. Results indicated that the PVT laminates reduces the thermal efficiency of a pure thermal collector by about 15% and a further 3.5% drop is found when electrical power is generated. The contribution of the thermal efficiency to the overall PVT panel efficiency is found to be the greatest at low coolant inlet tempera-ture but it strongly reduces as the coolant inlet temperature increases. Finally, the serpentine and the header riser configura-tions for the coolant circuit were compared finding that the latter achieves the highest overall performances.

All the previous studies provide valuable information about PVT solar collectors. The analysis of recent researches seems to state that PVT collectors with roll-bond absorber are the most suitable choice due to their higher performances. However, the experimental activity in this field is quite limited [14,16] and a comparison with traditional sheet-and-tube configuration is hardly found. As a result, strong conclusion about evident superiority of roll-bond configuration are difficult to be drawn and more data are needed for the sake of technologies comparison. Consequently, the aim of the present work is to experimentally compare three different PVT modules, in terms of both power and heat transfer rate: two

modules are PVT prototypes implementing a roll-bond absorber while the third is a commercial product based on sheet-and-tube concept and is used as the baseline. The difference between the two roll-bond prototypes lies in the insulation approach: the first adopts an innovative insulating coating, while the second is realized with a more conventional insulating material. In addition to the performance advantages previously discussed, the roll-bond configuration was adopted also because it is expected as one of the configurations with the lowest production cost since the roll-bond and the PV module can be produced separately with typical production processes and then connected together. The main drawback of this concept is the weight of the final system which is higher than that of the sheet and tube configuration (each mod-ule is about ten kg heavier). The experimental activities were car-ried out at the laboratory SolarTech^{LAB}, Politecnico di Milano during the summer season 2015 [18]. An important aspect dis-cussed in this work is about the index selection for the PVT perfor-mance assessment: a new index is here proposed and verified by the experimental activity.

The paper is organized as follows: In Section 2, the PVT modules considered in this work are described. Section 3 discusses the methodology adopted and the performance indexes which can be considered. Sections 4 and 5 present the experimental set-up and the uncertainty analysis. Results are presented in Section 6 and, finally, we conclude and outline additional research directions for future work in Section 7.

2. PVT modules

The experimental measurement were carried out to compare roll-bond configuration for PVT and a reference commercial PVT panel based on sheet and tube [19,20]. The reference PVT module is based on monocrystalline PV technology, while the roll-bond are applied to polycrystalline ones. Three different roll-bond PVT were experimentally characterized. Two of them, shown in Fig. 1, were provided with back insulation whereas the last one, without back insulation, was taken into consideration only for comparison, in order to evaluate the impact of the insulation on the perfor-mances of well-insulated roll-bond PVT collectors and, conse-quently, its results are not discussed.

The roll-bond design was kept constant in all the cases, while the sealant and/or the insulation technology were changed. The difference between the two back-insulated roll-bond PVT laid in the type of insulation adopted: the first one is realized with an insulating painting (referred to as RB1) and the second one with an insulating material (referred to as RB2). The characteristics of the sealant, insulation painting and material as well as roll-bond design are summarized in Table 1.

3. Methodology

PVT collectors produce simultaneously electric and thermal power, therefore their performances have to be compared both in terms of electric energy and heat produced during the experimental campaign.

The electric power P_{el} is directly measured by the micro-inverters and its value is used to calculate the electric efficiency according to the following definition:

$$\eta_{el} = \frac{P_{el}}{G \cdot A} \tag{1}$$

where G is the solar irradiance, which is directly measured by the pyranometer, and A is the panel nominal area.

On the other hand, the collector heat transfer rate is calculated from the measured values of the coolant inlet and outlet temperatures, and volumetric flow rate, according to the following equation:

$$\dot{Q}_{th} = \rho \dot{V} c (T_{out} - T_{in}) \tag{2}$$

where ρ and c are the coolant density and specific heat capacity, respectively.

While there is no discussion about the definition of the electric efficiency (Eq. (1)), there are two different definitions of thermal efficiencies (η_{th}, η^*_{th}) which can be adopted. Several authors [5,8,15,23,24] consider as energy input the entire solar radiation as shown in Eq. (3):

$$\eta_{th} = \frac{\dot{Q}_{th}}{G \cdot A} = \frac{\rho \dot{V} c (T_{out} - T_{in})}{G \cdot A} \tag{3}$$

Whereas in the second perspective, proposed and adopted in this work, the electric power generated is subtracted to the solar radiation as shown in Eq. (4):

$$\eta^*_{th} = \frac{\dot{Q}_{th}}{G \cdot A - P_{el}} = \frac{\rho \dot{V} c (T_{out} - T_{in})}{G \cdot A - P_{el}} = \frac{\eta_{th}}{1 - \eta_{el}} \tag{4}$$

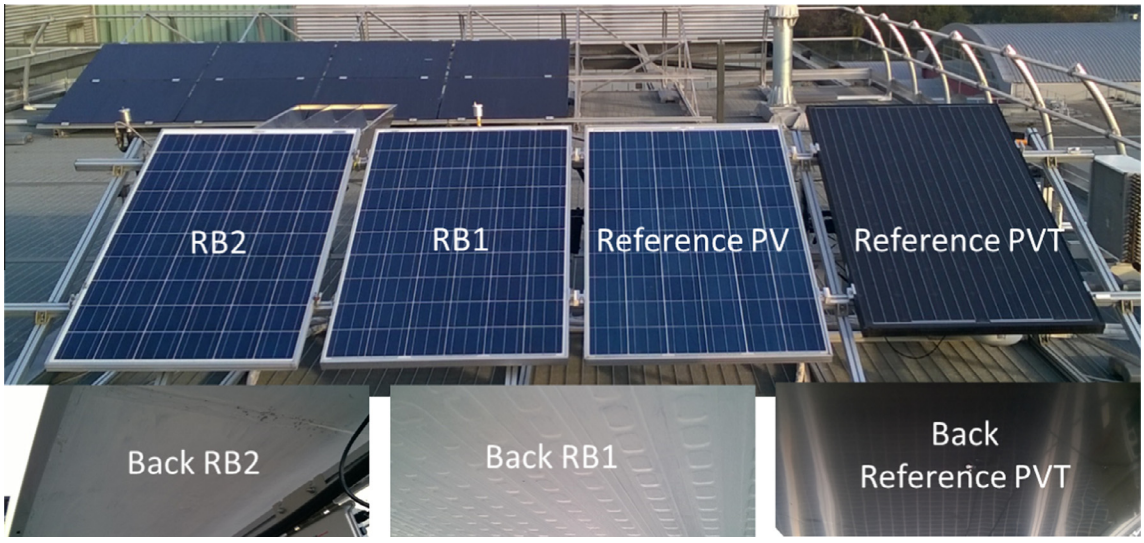

Fig. 1. PVT modules installed (front and back) @ Solartech^{Lab} and tested in this work.

Table 1
Summary of the three PVT modules considered in this work.

	REF	RB1	RB2
PV cell	Mono	Poly	Poly
Power output, W	245	245	245
Module size ($H_p \times L_p \times D_p$), mm	1660 × 990 × 40	1650 × 992 × 40	1650 × 992 × 40
Heat recovery system	Sheet&Tube	Roll-Bond	Roll-Bond
Material	Copper	Aluminum	Aluminum
Sealant	Not necessary	Terostat MS930 [21]	Loxeal 4826 [22]
Insulating material	NA	Insulating painting k = 0.1 W/mK Thickness = 1 mm	Insulating material k = 0.04 W/mK Thickness = 3 mm
Tubes/Passes	1/6	3/5	3/5

Table 2
Energy meter features and metrological characteristics.

Nominal voltage V_N	3 × 230/400 V_{AC} (direct insertion)
Current ratings	Maximum current I_{max}: 60 A_{AC} (direct insertion)
Measurement channels impedance	Voltage inputs: 1 MΩ Current inputs: negligible
Uncertainty	Active energy: class 1 Reactive energy: class 2

This new definition of thermal efficiency allows a fair comparison between PVT and solar thermal panels. In addition, the diverse PV cell technologies/efficiency can be decoupled from the thermal performances.

About thermal efficiency calculation, some authors [8,17] extended the typical linear dependency on reduced temperature of solar panels to the PVT concept according to the following equation:

$$\eta_{th} = \eta_{opt} \cdot IAM(1 - \eta_{el}) - K\frac{(T_{ave} - T_{amb})}{G} \quad (5)$$

In authors' opinion, this approach is not strictly correct, because the electric efficiency is affected by the absolute cell temperature, while the collector heat losses just depend on the temperature difference between the module and the ambient. Therefore, providing the optical and electric efficiency and K is just an approximation which will not be used in this work.

Moving to parameters which define the module overall performances, the simultaneous electricity and thermal production can be described by the total efficiency (also known as first law efficiency) which is the sum of electric and thermal efficiency where the latter is calculated according to Eq. (3):

$$\eta_I = \eta_{el} + \eta_{th} \quad (6)$$

With this approach, the electricity and heat have the same value. However, other studies [3,25] proposed to consider as overall performance index a modified primary energy savings (PES) which weights the electricity and heat with the reference generation technology, being the reference efficiency for electrical energy the average efficiency of power plants at national level:

$$PES = \eta_{th} + \frac{\eta_{el}}{\eta_{el,ref}} \quad (7)$$

In this work, a second law efficiency is also adopted as overall performance index. Having electricity and heat a different thermodynamic value, the thermal energy is weighed by means of the efficiency of an ideal process converting the heat into work.

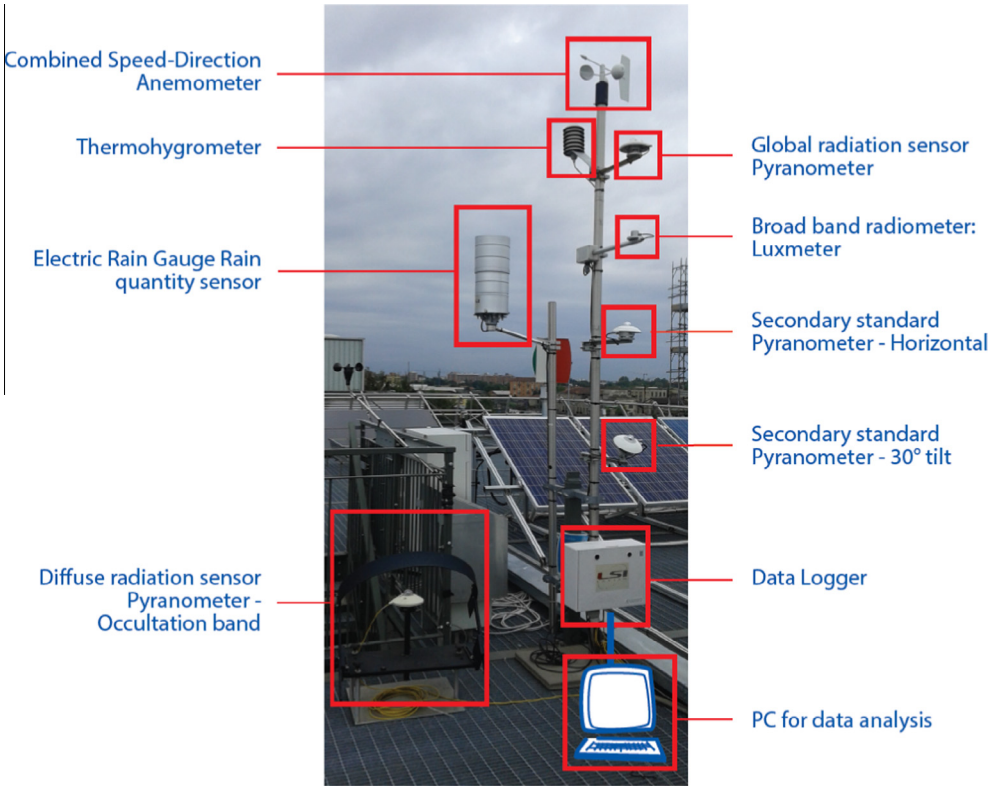

Fig. 2. Weather station and measurement system @ SolarTechLab.

$$\eta_{II} = \eta_{el} + \eta_{th} \cdot \eta_{ideal} \tag{8}$$

It is worth specifying that the ideal efficiency is evaluated with reference to the Lorentz cycle, and not to the Carnot cycle, because the heat produce by the PVT is available at variable temperature rather than at constant temperature. Consequently, the ideal efficiency is calculated as follows:

$$\eta_{ideal} = \frac{\int_{Tamb}^{Tout} cdT\left(1 - \frac{T_{amb}}{T}\right)}{\int_{Tamb}^{Tout} cdT} = 1 - \frac{T_{amb}}{T_{LMTD}} \tag{9}$$

The adoption of the second law efficiency is preferable, being this efficiency an absolute value, while the PES of the same module would vary from country to country because of the different reference efficiency for the electricity production, which is site dependent.

4. Experimental set-up

The experimental analysis was performed at the laboratory SolarTech^{LAB} [18], Politecnico di Milano, whose geographical coordinates are latitude 45°30′10.588″N and longitude 9°9′23.677″E. The experimental measurements are carried out in real operating conditions, so results are not intended to be of certification type. All the different technologies are tested at the same time, under the same environmental conditions, and using the same measure-ment instrumentation, so as to provide comparative analysis of performance.

A total of twenty-six pure photovoltaic or hybrid PVT modules are installed in the laboratory: ten monocrystalline collectors, eleven poly-crystalline collectors (from three different manufactures) and five hybrid (photovoltaic and thermal) PVT collectors. The rated power of the installed modules ranges from 75 to 300 W_P. The connection to the grid is carried out by micro inverters, one for each module. This configuration allows the electrical indepen-dence of each module and allows the optimization of the electricity production for each collector (pure PV or PVT). Therefore, the electric production of each PVT module under investigation can be controlled and saved independently outlining the advantage of the cooling effect or comparing different cooling technologies. The operating parameters of each micro inverter are transferred in real time, using wireless connection, to a PC for storage and further analysis. The energy flow between the PV (or PVT) collectors and the electrical grid are measured by an energy meter that equips each micro-inverter and whose characteristics are reported in Table 2.

Table 3
Solar irradiance and temperature sensor characteristics.

Irradiance sensors	Pyranometer (LSI, DPA252)
Standard	Secondary standard ISO 9060
Measurements range (W m^{-2})	<2000
Spectral range	300–3000 nm
Total achievable daily uncertainty	<2%
Directional response	<±5.4 W m^{-2}
Thermal drift	<2%
Temperature and humidity sensor (LSI, DMA 875)	
Temperature sensor	Pt100 1/3 B (DIN EN 60751)
Measurements range	[−30 °C, +70 °C]
Uncertainty	0.2 °C (at 0 °C)
Resolution	0.04 °C
Response time (T90)	3 min: with filter; 20 s: without filter (air speed 0.2 m s^{-1})

The environmental conditions are monitored with a meteorological station equipped with a solar irradiance sensor, temperature and humidity sensors, wind speed and direction sensor and rain collector. Solar irradiance is measured with two secondary standard pyranometers for the measurement of the total irradiance on horizontal and 30° tilt planes. In addition, a pyranometer with shadow band is available for measuring the diffuse irradiance. The pyranometer at 30° tilt is directly used to define the solar irradiation on the modules (G in Eqs. (1), (3) and (4)) which have the same tilt.

The main characteristics of the sensors together with the temperature measuring equipment are shown in Fig. 2 and reported in Table 3. The meteorological station performs ambient conditions measurements every ten seconds. The average, maximum,

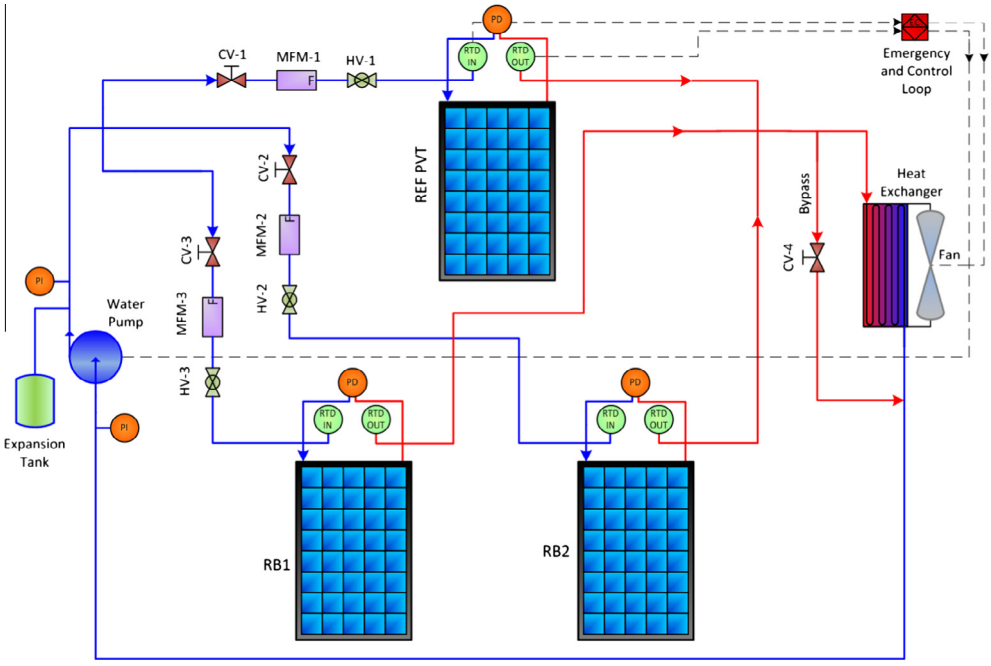

Fig. 3. Thermal loop at SolarTech^{LAB}.

Table 4
Characteristic of the main measurement system in the thermal loop.

Instruments	Thermoresistances	Flowmeters		Differential pressure transmitters
		REF/RB1	RB2	
Uncertainty	1/10 (DIN EN 60751)	±1% FS	±1% RV	±0.1% FS
Range	[−50 °C, 250 °C] rev1	0.9–15 l/min	0.25–9 l/min	3.2–320 mbar
Signal	RTD module adopted	4–20 mA		4–20 mA

Table 5
Uncertainty of heat transfer rate and thermal efficiency with different solar irradiance for RB1.

G [W m^{-2}]	$\dot{Q}_{TH}$ [W]	$U(\dot{Q}_{TH})$ [W]	$U_{\%}(\dot{Q}_{TH})$ [%]	η^*_{TH} [%]	$U(\eta^*_{TH})$ [%]	$U_{\%}(\eta^*_{TH})$ [%]
400	172.26	8.51	4.94	32.74	1.81	5.52
500	232.92	9.11	3.91	35.07	1.61	4.60
600	286.15	9.57	3.34	35.70	1.47	4.11
700	300.21	9.99	3.33	31.92	1.31	4.09
800	344.96	11.34	3.29	32.09	1.30	4.06
900	438.55	12.78	2.91	36.33	1.24	3.41

minimum and standard deviation of the values measured by the sensors are calculated every ten minutes and these values are stored into a database. These values are used for the evaluation of the performances of PVT collectors.

PVT modules are installed in a dedicated section of the laboratory. The cooling circuit consists of a pump, that feeds three different collectors in parallel, and a dry-cooler that closes the loop as shown in Fig. 3. All PVT modules are placed on the same structure to avoid differences in terms of incidence angle and the coolant mass flow rate at their inlet can be independently adjusted in order to achieve the desired thermal conditions (e.g. the same coolant temperature increase inside each collector).

Mass flow rates in each hydraulic circuit are measured by means of flow meters (MFM in Fig. 3) placed after the pump, temperatures at PVT inlet and outlet are measured using Pt-100 (1/10 DIN) RTDs (RTD in Fig. 3) and pressure differences by differential pressure transmitters (PD in Fig. 3). Main features of the thermal loop instrumentation are summarized in Table 4.

A National Instrument™ cRIO rack is used for data acquisition; data are sent via LAN to a host PC where a LabVIEW™ program is used to read, visualize, analyze and store the measurements. Data are read every second and their average and standard deviation on minute basis are saved in a file for further analysis and elaboration.

5. Uncertainty analysis

Thermal loop data are acquired every second. In order to reduce the uncertainty related to every single measurement, the mean value of sixty samples (minute average) is computed. Accordingly, the uncertainty can be computed using Eq. (10).

$$U(x_j) = \sqrt{U_B^2(x_j) + \frac{\sigma_{st}^2(x_j)}{N}} \tag{10}$$

As all the instruments were calibrated before the experiments, the first term in the square root is zero. According to the uncertainty propagation theory, and assuming that: x_i is one of N measured quantity, whose absolute uncertainty is $U(x_i)$, $U(x_i)$ is a random variable not related to the others and that the quantity y depends on the N measured quantities x_i: $y = y(x_1, x_2, \ldots, x_j, \ldots, x_M)$, the absolute uncertainty U(y) can be computed Eq. (11):

$$U(y) = \sqrt{\sum_{j=1}^{M} \left(\frac{\partial f}{\partial x_j}\right)^2 \cdot U(x_j)^2} \tag{11}$$

With this equation it is possible to calculate $U(\dot{Q}_{th,i})$ and $U(\eta^*_{th,i})$ by using the following expressions:

$$U_{\%}(\dot{Q}_{th,i}) = \sqrt{U_{\%}(\dot{V})^2 + \frac{2}{\Delta T_i^2} U(T)^2} \tag{12}$$

$$U_{\%}(\eta^*_{th,i}) = \sqrt{U_{\%}(\dot{V})^2 + \frac{2}{\Delta T_i^2} U(T)^2 + \frac{1}{(1-\eta_{el,i})^2}\left[U_{\%}(G_i)^2 + \eta_{el,i}^2 \cdot U_{\%}(P_{el,i})^2\right]} \tag{13}$$

Uncertainty of daily heat transfer rate and thermal efficiency is obtained, in accordance with Eq. (11), by:

$$U_{\%}(\dot{Q}_{th}) = \sqrt{\frac{2}{N\Delta T_m^2} U(T)^2 + U_{\%}(\dot{V})^2 + U_{\%}(\Delta t)^2} \tag{14}$$

$$U_{\%}(\eta^*_{th}) = \sqrt{U_{\%}(\dot{V})^2 + \frac{2U(T)^2}{N\Delta T_m^2} + \left(\frac{\eta_{el,m}}{1-\eta_{el,m}}\right)^2 \left[\left(\frac{N-1}{N^2}\frac{G_s^2}{G_m^2} + 1\right)\left[\frac{U_{\%}(G)}{\eta_{el,m}}\right]^2 + \frac{N-1}{N^2}\frac{P_{el,s}^2}{P_{el,m}^2} + 1\right) U_{\%}(P_{el})^2\right]} \tag{15}$$

where both sums are extended to all of the available daily minute average values.

In order to give an idea about the uncertainties of the average thermal power and efficiency on minute base, their values at different solar radiations for RB1 module are shown in Table 5 where it is possible to observe that the increase of solar irradiance reduces the relative uncertainty, according to the reduction of the standard deviation.

The uncertainty can be reduced by using significant number of samples to calculate the average power and efficiency. As already

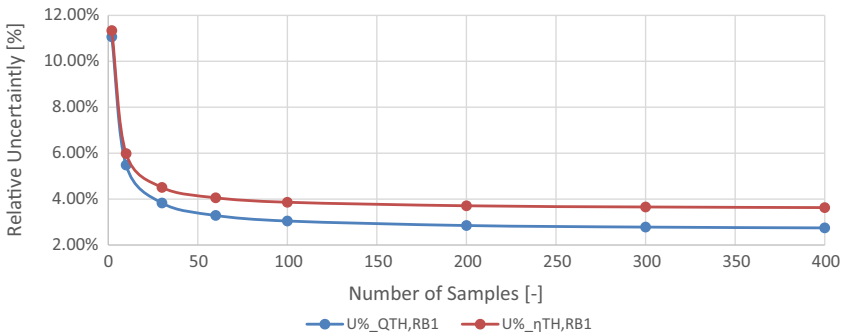

Fig. 4. Relative uncertainty of heat transfer rate and thermal efficiency as a function of the number of samples with 800 W m^{-2} of solar irradiance.

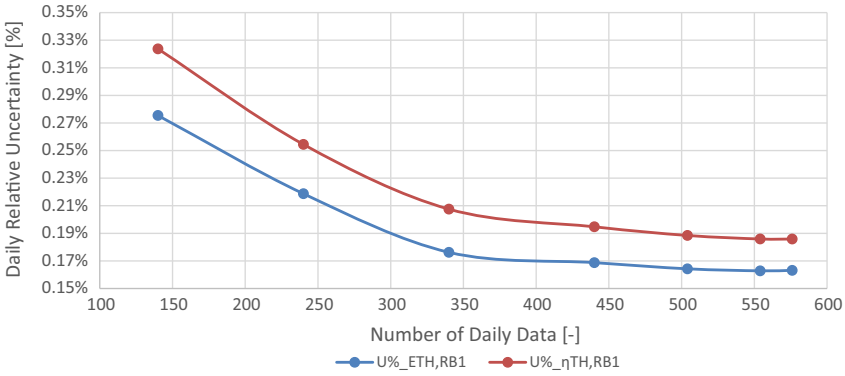

Fig. 5. Relative uncertainty of heat transfer rate and thermal efficiency as a function of the number of daily data.

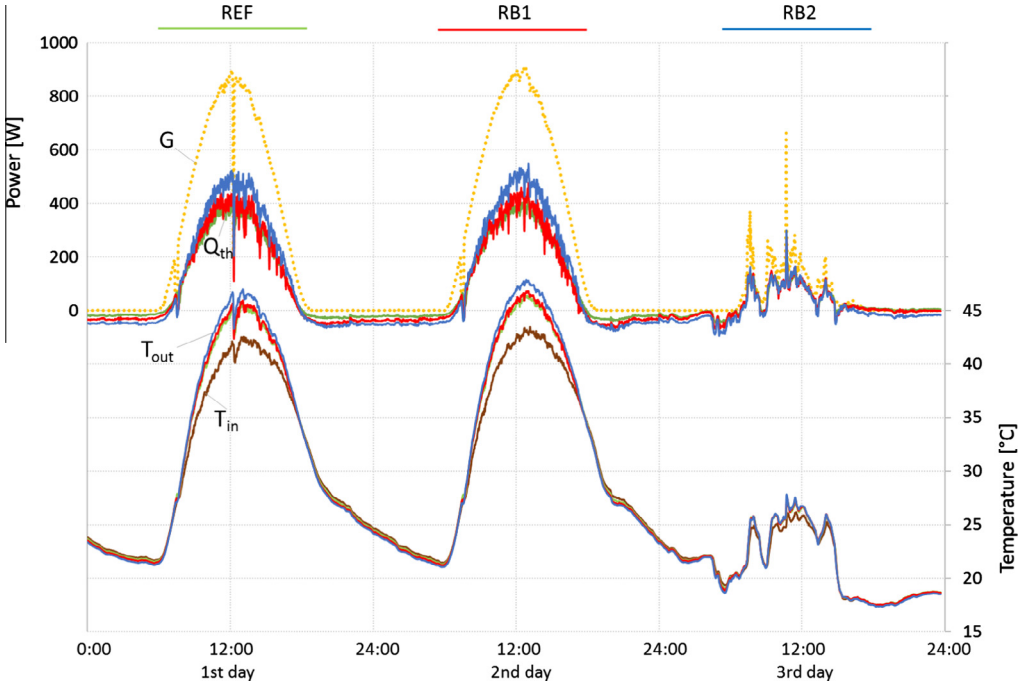

Fig. 6. Performances (heat transfer rates and temperature) of the three considered PVT modules in two sunny and one cloudy day (the dashed line is G).

Table 6
Electric and thermal performances of the considered PVT.

Day	I_{TOT} [kW h m^{-2}]	$E_{EL,TOT}$ [kW h]				$E_{TH,TOT}$ [kW h]		
		PV	Ref	RB1	RB2	Ref	RB1	RB2
02/07/2015	4.73	1.06	1.08	1.15	1.16	1.43	2.29	2.82
03/07/2015	4.99	1.12	1.13	1.21	1.23	1.61	2.59	3.03
05/08/2015	5.23	1.18	1.18	1.27	1.28	2.49	2.39	2.86
06/08/2015	5.84	1.30	1.31	1.41	1.41	2.60	2.48	3.08
07/08/2015	5.80	1.29	1.30	1.39	1.39	2.60	2.48	3.04
08/08/2015	6.08	1.35	1.36	1.46	1.46	2.73	2.65	3.17
20/08/2015	3.34	0.75	0.75	0.81	0.82	1.36	1.44	1.72
27/08/2015	4.81	1.08	1.08	1.17	1.17	2.06	2.21	2.66
29/08/2015	5.39	1.21	1.20	1.31	1.27	2.29	2.42	2.95
31/08/2015	5.44	1.21	1.21	1.31	1.27	2.19	2.29	2.85
02/09/2015	3.81	0.85	0.86	0.94	0.94	1.61	1.63	2.02
08/09/2015	1.02	0.26	0.25	0.27	0.27	0.48	0.31	0.30
Overall	58.48	12.65	12.72	13.70	13.67	23.44	25.19	30.50

mentioned, in this work the parameters are measured every second, but the minute average is considered. This is reasonable when looking at Fig. 4, where, in accordance with Eqs. (14) and (15), the relative uncertainty reduces to 4% for a number of samples N = 60.

Finally, the overall comparison between the different PVT modules is carried out on daily performances. Fig. 5 explains the dependence of daily relative uncertainty from the number of daily data used starting from the minute average. As the previous case, the uncertainty decrease with high numbers of data. The figure also shows that daily uncertainty can be negligible and it won't affect the performance comparison of the considered PVT modules. For this reason, it won't be shown in the final table.

6. Results

In this section the performance of the three PVT modules is discussed. The experimental tests are carried out with the same water inlet temperature for the three PVT panels while the water flow rate of each PVT module is set at typical values (about 1.65 l/min for module). It must be reminded that the set-up was designed to determine the PVT module performances under real operating conditions, being the steady-state performances provided by manufacturer in their datasheets.

Heat transfer rates together with average inlet and outlet water temperatures on a minute basis for selected days, featuring sunny and cloudy conditions, are reported in Fig. 6. In general, RB2 has the highest heat transfer rate together with the highest outlet temperature. The fluid temperature variation is in the range of 5 °C for RB2 at 900 W m^{-2} and 40 °C temperature inlet, while no temperature differences between inlet and outlet can be seen for G below 250 W m^{-2}. The heat transfer rate at 900 W m^{-2} is between 400 W (REF and RB1) and 500 W for RB2. During cloudy days, there is some heat transfer rate even at low radiations, but at temperatures around 25 °C. Finally, the heat transfer is negative during night time as consequence of the heat losses and lack of solar radiation. It can be noted that the experimental setup has limited inertia since the thermal loop consists only of three PVT panels without any storage tank, leading to almost instantaneous temperature variations as soon as solar radiation changes or wind blows (i.e.

Table 7
Thermal performances of the considered PVT when non electric power production takes place.

Day	I_{TOT} [kW h m^{-2}]	$E_{TH,TOT}$ [kW h]		
		Ref	RB1	RB2
04/07/2015	4.39	1.31	2.04	2.57
10/07/2015	0.66	0.38	0.36	0.47
11/07/2015	6.31	3.25	2.72	3.70
12/07/2015	5.88	3.34	3.30	4.07
21/07/2015	5.30	2.86	2.59	3.45
22/07/2015	5.18	2.78	2.59	3.36
23/07/2015	4.99	2.59	2.37	3.16
24/07/2015	5.46	3.04	2.92	3.57
28/07/2015	3.89	2.31	2.33	2.75
02/08/2015	4.62	2.75	2.83	3.38
03/08/2015	5.39	2.94	2.93	3.59
Overall	52.07	27.55	26.99	34.08

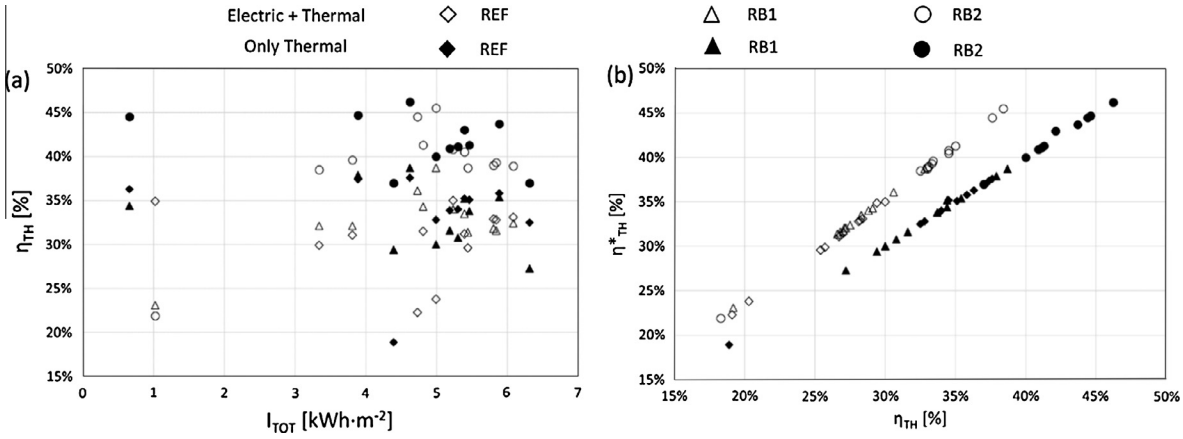

Fig. 7. Standard thermal efficiency versus overall radiation (a) and modified thermal efficiency versus standard thermal efficiency (b).

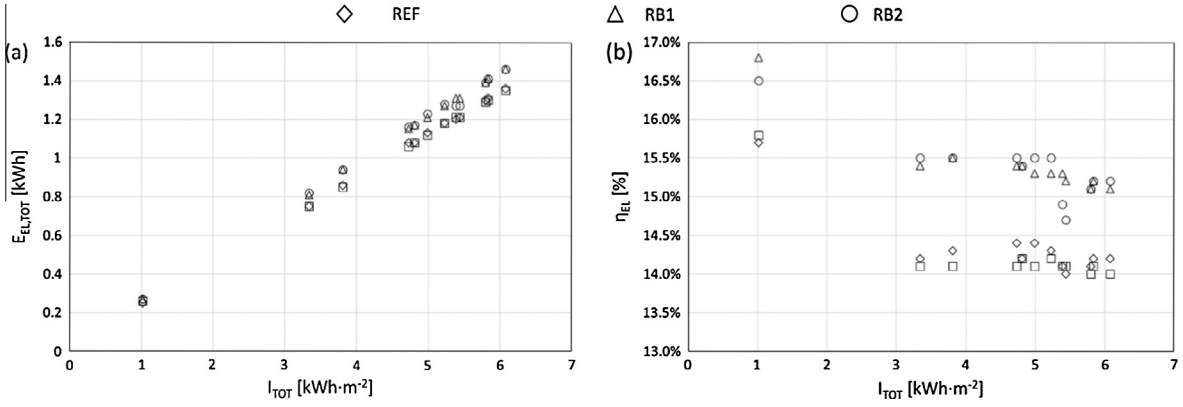

Fig. 8. Electric energy output of the PVT (a) and electric efficiency (b) of the PVT modules.

in Fig. 6, both solar irradiation and temperatures drop around mid-day of the first day or look at the general trend in the third day).

For a consistent and fair comparison, the diverse thermal inertia, consequence of different materials and thicknesses of the PVT, must be taken into account: REF module inertia is lower than those of RB1 and RB2. Consequently, the most appropriate compar-ison among the three PVT panels is performed considering the energy performances on a daily basis, assuming equal initial and final temperatures, instead of instantaneous thermal power.

Daily energy performances of the two considered PVT collectors with roll-bond are reported in Tables 6 and 7 (only production of thermal power without any electric power, i.e. disconnected inverters), together with the ones of the reference sheet-and-tube PVT collector for several days and, for the sole Table 6, with data from a pure PV collector. Calculations are carried out assum-ing an initial and final temperatures of 36 ° C for all the considered modules. Assuming different temperature will not change results in relative terms. Data show that the PVT collectors perform better than the pure PV one due to the cooling effect of water loop that reduces the cell temperature. Moreover, performance of roll-bond collectors are higher with respect to the baseline PVT one due to a better heat extraction of the roll-bond absorber: the sur-face over which the cold water flows is larger. Finally, RB2 achieves higher thermal performance with respect to RB1, due to the better back insulation, and similar electric efficiency.

Fig. 7(a)[2] shows the thermal efficiency of the three modules as function of the daily solar radiation either for the situation when both electric and thermal power are produced (empty markers) and for the situation when only thermal power is produced (full markers). RB2 panel seems to have the highest thermal perfor-mances while the REF and RB1 collectors have a similar behavior. This suggests that the RB1 suffers higher thermal losses and, consequently, that the adoption of roll-bond as heat recovery technology can be more efficient than sheet-and-tube configuration only if combined with adequate insulating material. Moreover, RB1 has a thermal efficiency comparable with REF when the module produces electricity, while the situation changes when the power production is switched off, in this case REF seems to have better performances. This suggests that the RB1 exhibits higher thermal losses when the temperature difference between the PV module and the ambient increases. Finally, RB configuration performs better at high irradiation, while REF exceeds RBs in days with irradiation between 1 and 2 kW h/m^2 day (08/09 and 10/07). This is supposed to be related to the highest heat capacity of roll-bond collectors that leads to a reduction in the heat transfer between the panel and the coolant. Overall, the average thermal efficiency without electricity produc-tion ranges from 33% to 41% which is 25% points lower than flat plate thermal panels operating under the same average temperatures and radiations.[3]

A comparison between the thermal efficiencies of the three modules defined in the standard mode, (see Eq. (3)), and the one introduced in the present paper, calculated according to Eq. (4), is shown in Fig. 7(b).[4] Generally speaking, when the PVT produces electrical and thermal energy simultaneously, the modified thermal efficiency is point by point higher than the conventional one, with differences ranging from 3% to 7%, according to its definition. Vice versa, when the PVT collectors do not produce any electric power, the two efficiency are exactly equal.

Focusing on the electric efficiency, the adoption of a heat recovery system which acts as coolant for the PV cells allows higher con-

Table 8
First and second law efficiencies of the three considered PVT.

Day	I_{TOT} [kW h m^{-2}]	P_{el}	η_I			η_{II}		
			REF	RB1	RB2	REF	RB1	RB2
02/07/15	4.73	Y	33.4	45.9	53.2	15.1	16.6	17.0
03/07/15	4.99	Y	34.7	48.0	53.9	15.2	16.5	17.0
03/08/15	5.39	Y	44.3	44.1	49.9	15.8	16.6	16.5
05/08/15	5.23	Y	42.3	42.0	48.5	15.4	16.4	16.0
06/08/15	5.84	Y	42.4	42.2	48.3	15.3	16.3	16.0
07/08/15	5.80	Y	42.5	42.7	48.1	15.3	16.2	16.2
08/08/15	6.08	Y	39.9	42.6	48.0	15.3	16.7	17.0
20/08/15	3.34	Y	41.3	44.5	50.4	15.4	16.6	16.8
27/08/15	4.81	Y	40.9	43.7	49.4	15.3	16.5	15.5
29/08/15	5.39	Y	39.4	41.8	47.8	15.0	16.3	15.1
31/08/15	5.44	Y	40.9	42.6	49.0	15.6	17.1	16.9
08/09/15	1.02	Y	45.2	36.1	34.8	18.2	18.6	18.2
Overall	58.48	Y	40.4	43.5	49.4	15.6	16.7	16.5
04/07/15	4.39	N	18.9	29.4	37.0	0.6	1.1	1.4
10/07/15	0.66	N	36.3	34.5	44.5	1.7	1.6	2.2
11/07/15	6.31	N	32.5	27.3	37.1	1.5	1.3	1.8
12/07/15	5.88	N	35.9	35.5	43.7	1.4	1.5	1.8
21/07/15	5.30	N	34.0	30.9	41.2	1.4	1.3	1.8
22/07/15	5.18	N	33.9	31.6	40.9	1.4	1.3	1.8
23/07/15	4.99	N	32.8	30.1	40.1	1.5	1.4	1.9
24/07/15	5.46	N	35.2	33.8	41.3	1.4	1.3	1.7
28/07/15	3.89	N	37.4	38.0	44.7	1.5	1.5	1.8
02/08/15	4.62	N	37.6	38.7	46.3	1.9	1.9	2.4
03/08/15	5.39	N	34.5	34.4	42.1	1.9	2.1	2.3
Overall	52.07	N	33.4	32.7	41.3	1.5	1.5	1.9

version efficiencies with respect to reference PV modules (Fig. 8). In general, the RB configuration allows a more uniform tempera-ture distribution on the entire module than the sheet-and-tube one due to the higher number of tubes where coolant flows, hence the cell temperature reduces with efficiency advantages. It is important to stress that PV cell are connected in series, so even limited hot zones may penalize the entire module performances.

Fig. 8[5] highlights also that the solar irradiance slightly affects the electric efficiency justifying the alignment of thermal and electric power in Fig. 7: if the electric efficiency is constant the thermal efficiency and the modified thermal efficiency are proportional (see Eq. (4)).

The first and second law efficiencies as well as the overall values are summarized in Table 8. The first law efficiency is higher with electricity production and it is between 40% and 49%, reducing the performance difference between PVT and conventional thermal panels. The situation completely changes when considering the second law efficiency where the thermal power has limited contribution since the Lorentz efficiency is very low, below 10%, due to low coolant inlet and outlet temperature (roughly between 30 °C and 45 °C). Assuming the second law perspective, the adoption of combined heat and power generation is fully justified. Besides first and second law efficiencies, the economic value of thermal and electric power is fundamental to determine whether additional investments can be balanced by the higher revenues.

Together with thermal performances of different panels, pressure drops were also monitored providing an idea about differences and limitation to the lay-out (series vs. parallel configurations) of a PVT solar field. The pressure drop of the reference PVT is equal to 3000 Pa at typical operating conditions (mass flow rate equal to 2 l/min, average coolant temperature equal to 35 ° C) whereas the roll-bond configuration shows significantly higher pressure drop, reaching 7000 Pa at the same operating conditions. This higher value must be taken into account when defining the recovery lay-out: in a PVT solar field a limited number of roll-

[2] For actual values see table A in supplementary material.

[3] The reference panel is based on flat plate collectors with η_0 and K equal to 0.75 (including fouling) and 4 W m^{-2} K^{-1} respectively, average G 674 W m^{-2}, ambient temperature 27.4 °C and average module temperature of 41 °C.

[4] For actual values, see table A in supplementary material.

[5] For actual values, see table B in supplementary material.

bond based PVT can be placed in series, limiting the maximum outlet temperature.

7. Conclusions

In this paper, three different PVT modules were tested at the SolarTech^{LAB}. The performance of two innovative PVT prototypes, adopting roll-bond technology as heat recovery concept, were compared to the performance of a commercial PVT module, based on a conventional sheet-and-tube concept, that acted as the baseline.

Experimental activities were carried out in real operating: the performance assessment was carried out considering daily performance as terms of comparison between the different technologies. The results showed that roll-bond modules can reach higher thermal efficiency than sheet-and-tube configuration provided that an adequate insulation is added to collector bask. The thermal efficiency can increase by about 10% points with even slightly higher electricity production. The resulting first law and second law efficiency can be as high as 49% and 16.2% for the best roll-bond, while the baseline module achieves thermal and electrical efficiencies equal only to 40% and 15.6% respectively. Thanks to this extensive experimental campaign, the potentiality of roll bond as heat recovery technology applied to PV modules is confirmed. Additional experiments are on-going to investigate and optimize the insulation and see how the performances of roll-bond modules can be further improved.

A second finding of the work is found in the performance assessment, where new indexes are proposed. Besides the electric and thermal efficiencies, typically adopted in conventional PV and thermal panel analysis, additional parameters are introduced to account for PVT peculiarities and make consistent comparisons. The validity of the proposed thermal efficiency correction, by means of the electric power produced, was confirmed by the experimental analysis. Finally, the second law analysis outlined the potentiality of PVT covering the gap with the conventional thermal panels: the higher thermodynamic value of electricity more than balance the lower thermal efficiency.

Acknowledgements

The presented work was partially funded within the ETICO project by the "MINISTERO PER LO SVILUPPO ECONOMICO" within the RIDITT framework Progetto n. 56 - CUP B45E11001050008. Note: "The present publication reflects only the authors' views and the MINISTERO PER LO SVILUPPO ECONOMICO are not liable for any use that may be made of the information contained therein". The authors would like to thank SMERI srl for supplying the instrumentation.

Appendix A. Supplementary data

Supplementary data associated with this article can be found, in the online version, at http://dx.doi.org/10.1016/j.applthermaleng.2016.05.172.

References

[1] M.S. Buker, S.B. Riffat, Building integrated solar thermal collectors – a review, Renew. Sustain. Energy Rev. 51 (2015) 327–346, http://dx.doi.org/10.1016/j.rser.2015.06.009.
[2] H.A. Zondag, D.W. De Vries, W.G.J. Van Helden, R.J.C. Van Zolingen, The yield of different combined PV-thermal collector designs, Sol. Energy 74 (2003) 253–269.
[3] N. Aste, C. del Pero, F. Leonforte, Water flat plate PV-thermal collectors: a review, Sol. Energy 102 (2014) 98–115, http://dx.doi.org/10.1016/j.solener.2014.01.025.
[4] A. Kumar, P. Baredar, U. Qureshi, Historical and recent development of photovoltaic thermal (PVT) technologies, Renew. Sustain. Energy Rev. 42 (2015) 1428–1436, http://dx.doi.org/10.1016/j.rser.2014.11.044.
[5] X. Zhang, X. Zhao, S. Smith, J. Xu, X. Yu, Review of R&D progress and practical application of the solar photovoltaic/thermal (PV/T) technologies, Renew. Sustain. Energy Rev. 16 (2012) 599–617, http://dx.doi.org/10.1016/j.rser.2011.08.026.
[6] W.A. Duffie, J.A. Beckman, Solar Engineering of Thermal Processes, second ed., John Wiley & Sons Inc., New York, 1991.
[7] S.C. Solanki, S. Dubey, A. Tiwari, Indoor simulation and testing of photovoltaic thermal (PV/T) air collectors, Appl. Energy 86 (2009) 2421–2428, http://dx.doi.org/10.1016/j.apenergy.2009.03.013.
[8] T.T. Chow, A review on photovoltaic/thermal hybrid solar technology, Appl. Energy 87 (2010) 365–379, http://dx.doi.org/10.1016/j.apenergy.2009.06.037.
[9] R. Daghigh, M.H. Ruslan, K. Sopian, Advances in liquid based photovoltaic/thermal (PV/T) collectors, Renew. Sustain. Energy Rev. 15 (2011) 4156–4170, http://dx.doi.org/10.1016/j.rser.2011.07.028.
[10] A. Ibrahim, M.Y. Othman, M.H. Ruslan, S. Mat, K. Sopian, Recent advances in flat plate photovoltaic/thermal (PV/T) solar collectors, Renew. Sustain. Energy Rev. 15 (2011) 352–365, http://dx.doi.org/10.1016/j.rser.2010.09.024.
[11] V.V. Tyagi, S.C. Kaushik, S.K. Tyagi, Advancement in solar photovoltaic/thermal (PV/T) hybrid collector technology, Renew. Sustain. Energy Rev. 16 (2012) 1383–1398, http://dx.doi.org/10.1016/j.rser.2011.12.013.
[12] M. Herrando, C.N. Markides, K. Hellgardt, A UK-based assessment of hybrid PV and solar-thermal systems for domestic heating and power: system performance, Appl. Energy 122 (2014) 288–309, http://dx.doi.org/10.1016/j.apenergy.2014.01.061.
[13] J. Ji, H. He, T. Chow, G. Pei, W. He, K. Liu, Distributed dynamic modeling and experimental study of PV evaporator in a PV/T solar-assisted heat pump, Int. J. Heat Mass Transf. 52 (2009) 1365–1373, http://dx.doi.org/10.1016/j.ijheatmasstransfer.2008.08.017.
[14] P. Dupeyrat, C. Menezo, H. Wirth, M. Rommel, Improvement of PV module optical properties for PV-thermal hybrid collector application, Sol. Energy Mater. Sol. Cells 95 (2011) 2028–2036, http://dx.doi.org/10.1016/j.solmat.2011.04.036.
[15] J. Kim, J. Kim, The experimental performance of an unglazed PV-thermal collector with a fully wetted absorber, Energy Procedia 30 (2012) 144–151, http://dx.doi.org/10.1016/j.egypro.2012.11.018.
[16] N. Aste, F. Leonforte, C. Del Pero, Design, modeling and performance monitoring of a photovoltaic – thermal (PVT) water collector, Sol. Energy 112 (2015) 85–99, http://dx.doi.org/10.1016/j.solener.2014.11.025.
[17] J. Allan, Z. Dehouche, S. Stankovic, L. Mauricette, Performance testing of thermal and photovoltaic thermal solar collectors, Energy Sci. Eng. 3 (2015) 310–326, http://dx.doi.org/10.1002/ese3.75.
[18] SolarTech Lab, 2013. <www.solartech.polimi.it> (accessed 01.12.15).
[19] S. Buiani, E. Miani, Photovoltaic plant, 1 873 843 B1, 2010.
[20] Fototherm, 2015. <http://www.fototherm.com/en/fototherm-al-series.html> (accessed 01.11.15).
[21] Teroson MS 930, 2015. <http://www.henkelna.com/product-search-1554.htm?nodeid=8801991655425> (accessed 01.11.15).
[22] Loxeal 4826, 2015. <http://www.loxeal.com/files/tech_info_01_15_english.pdf> (accessed 01.11.15).
[23] R. Liang, J. Zhang, L. Ma, Y. Li, Performance evaluation of new type hybrid photovoltaic/thermal solar collector by experimental study, Appl. Therm. Eng. 75 (2015) 487–492, http://dx.doi.org/10.1016/j.applthermaleng.2014.09.075.
[24] G.M. Tina, A.D. Grasso, A. Gagliano, Monitoring of solar cogenerative PVT power plants: overview and a practical example, Sustain. Energy Technol. Assess. 10 (2015) 90–101, http://dx.doi.org/10.1016/j.seta.2015.03.007.
[25] B.J. Huang, T.H. Lin, W.C. Hung, F.S. Sun, Performance evaluation of solar photovoltaic/thermal systems, Sol. Energy 70 (5) (2001) 443–448, http://dx.doi.org/10.1016/S0038-092X(00)00153-5.